Journal of Nuclear Materials 377 (2008) 496–500

Contents lists available at ScienceDirect

Journal of Nuclear Materials

journal homepage: www.elsevier.com/locate/jnucmat

Characterization of creep–fatigue in ferritic 9Cr–1Mo–V–Nb steel using ultrasonic velocity

Chung Seok Kim [a], S.I. Kwun [a], Ik Keun Park [b,*]

[a] Division of Materials Science and Engineering, Korea University, Seoul 136-701, Republic of Korea
[b] Department of Mechanical Engineering, Seoul National University of Technology, 172, Gongreung 2-dong, Nowon-gu, Seoul 139-743, Republic of Korea

ARTICLE INFO

Article history:
Received 18 August 2007
Accepted 10 April 2008

PACS:
81.70.Cv
43.25.Ba
62.20.M

ABSTRACT

The microstructural evolution of ferritic 9Cr–1Mo–V–Nb steel, subjected to creep–fatigue at 550 °C, was evaluated nondestructively by measuring the ultrasonic velocity. The ultrasonic velocity was strongly depended on the microstructural changes during creep–fatigue. The variation in the ultrasonic velocity with the fatigue life fraction exhibited three regions. In the first region (within 0.2 N_f), a significant increase in the velocity was observed, followed by a slight increase between the fatigue life fractions of 0.2 N_f and 0.8 N_f and a decrease in the final region. The change of the ultrasonic velocity during creep–fatigue was interpreted in relation to the microstructural properties. This study proposes an ultrasonic nondestructive evaluation method of quantifying the level of damage and microstructural change during the creep–fatigue of ferritic 9Cr–1Mo–V–Nb steel.

1. Introduction

Ferritic 9–12%Cr steels designed for elevated temperature service have been recognized as a key material for the power generating industries. The high chromium content of these steels increases their oxidation resistance so that they can be utilized at higher temperatures than low alloy steels such as 1Cr–0.5Mo or 2.25Cr–1Mo steels. An improvement in the mechanical properties of modified 9Cr–1Mo steel was obtained by the addition of a small amount of niobium and vanadium, which are strong carbide formers and solid solution strengtheners.

Although these materials are continuously being developed to improve their mechanical properties, they generally undergo a softening of the matrix during their exposure to creep and fatigue at high temperature, due to the coarsening of the precipitates, the recovery of the dislocations and the depletion of the solute atoms from the matrix [1–3]. Therefore, in order to ensure the integrity and service life of these structural components, it is essential to understand their mechanical properties on the microstructural level.

Since it is sometimes impossible to take samples for analysis in the case of the structures in service, many researchers have attempted to evaluate the damage to such structures nondestructively by in situ monitoring. Ultrasonic [4–6], magnetic [7] and acoustic emission (AE) methods [8] are currently used for the nondestructive evaluation of structures. The method based on ultrasonic waves is applicable for the assessment of various kinds of bulk materials [4–6] because these waves (longitudinal or shear waves) can propagate through the whole thickness of the test material and provide much information on its characteristics. The present study describes the nondestructive evaluation of the creep–fatigue of ferritic 9Cr–1Mo–V–Nb steel by measuring the ultrasonic velocity.

2. Experimental procedure

The chemical composition of the ferritic 9%Cr steel used in this study is shown in Table 1. The material was supplied by Posco specialty steel, and had been normalized at 1050 °C and air cooled, followed by tempering at 760 °C for 1 h. The creep–fatigue test was conducted under load control in air using a servo-hydraulic fatigue test machine with a resistance heating furnace. The hold time at the maximum tensile stress (187 MPa) was either 60 s or 600 s. The temperature along the gauge length of the specimen was controlled to better than ±1 °C. Cylindrical specimens with a gauge length of 16 mm, a diameter of 10 mm and a shoulder radius of 20 mm were prepared. The interrupt test was conducted under the same creep–fatigue conditions to obtain coupons with different levels of creep–fatigue damage. The interruption times were chosen so that the ratio of the number of fatigue cycles to the total fatigue life (i.e. N/N_f) would be 0.1, 0.2, 0.4, 0.6 and 0.8.

An immersion technique was employed for the accurate measurement of the ultrasonic velocity. The ultrasonic measurement system used in this experiment consisted of a pulser/receiver for pulsating waves, a digital storage oscilloscope for analog/digital

* Corresponding author. Fax: +82 2 977 6332.
E-mail address: ikpark@snut.ac.kr (I.K. Park).

0022-3115/$ - see front matter © 2008 Elsevier B.V. All rights reserved.
doi:10.1016/j.jnucmat.2008.04.012

Table 1
Chemical composition of ferritic 9Cr–1Mo–V–Nb steel (wt%)

C	Si	Mn	P	S	Ni	Cr	Mo	Cu	V	Al	N	Nb	Fe
0.09	0.23	0.38	0.015	0.013	0.065	8.66	0.90	0.04	0.21	0.01	0.035	0.07	Bal.

conversion, a piezoelectric longitudinal broad band transducer with a center frequency of 23 MHz, an immersion tank with a parallelism-adjustment unit and a personal computer with commercial software for data acquisition and signal processing.

The microstructural observation was performed using field emission scanning electron microscopy (FESEM) after etching with Vilella's reagent. Electrolytic extraction was carried out to identify the precipitates by dissolving the matrix in 10% hydrochloric acid in methanol at a voltage of 3 V. The extracted residues were identified by X-ray diffraction (Cu Kα radiation). In order to examine the morphology and structure of the precipitates in detail, a carbon extraction replica was prepared and examined by transmission electron microscopy (TEM). In order to observe the dislocation substructures, thin foils were prepared by twin jet polishing in a solution of 25% perchloric acid at −15 °C and 60 V. The lath width was quantitatively measured from the TEM micrographs by the line intersection method for about 150 laths for each specimen. The dislocation density was measured from the X-ray line broadening using the Hall–Williamson method [9]. The X-ray diffraction patterns were obtained using a high resolution X-ray diffractometer with monochromatic Cu $K\alpha_1$ radiation at 40 kV and 25 mA.

3. Results

The variation in the ultrasonic velocity with the fatigue life fraction exhibited three regions, as shown in Fig. 1. A significant increase in the velocity was observed within 0.2 N_f (i.e. region I), followed by a slight increase between 0.2 N_f and 0.8 N_f (i.e. region II) and a decrease in the final region (i.e. region III).

The as-tempered specimen exhibited a martensitic structure with a high dislocation density in the lath interior and fine precipitates on the prior austenite grain (PAG) boundaries and martensite lath boundaries, as shown in Figs. 2(a) and 3(a). Fig. 2 represents the typical TEM micrographs showing precipitate morphology of as-tempered and fatigue fractured specimens. The number of cycles to fatigue failure was 3300 cycles for a tensile hold time of 60 s and 950 cycles for a tensile hold time of 600 s. The size of the precipitate increased slightly after fatigue failure at both stress hold times.

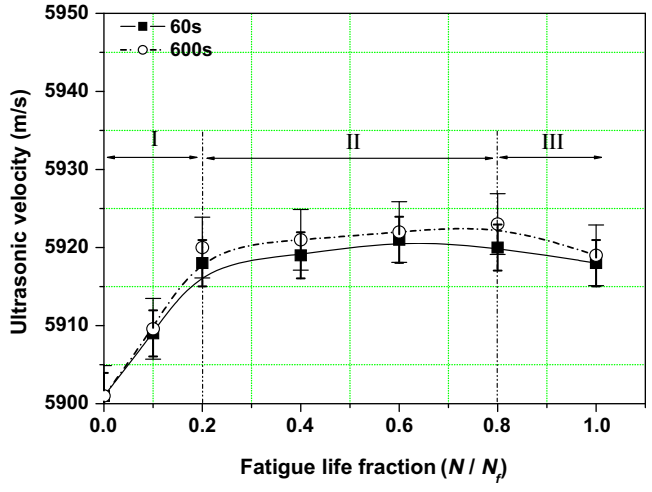

Fig. 1. Variation in the ultrasonic velocity with fatigue life fraction of ferritic 9Cr–1Mo–V–Nb steel.

Fig. 3 shows the typical TEM micrographs representing the dislocation substructure of as-tempered and fatigue fractured specimens. The dislocation density in the martensite lath interior decreased during creep–fatigue in the case of both stress hold times. Fig. 3(a) shows the presence of many elongated martensite lath structures. The dislocations within the martensite laths were tangled and their density was high. Fig. 3(b) and (c) show the microstructure after fatigue failure. The martensite lath width increased continuously during creep–fatigue, and the dislocation density within the lath interior was lower than that in Fig. 3(a).

Fig. 4 presents the typical backscattered electron (BSE) micrographs showing the surface morphology of the as-tempered and fatigue fractured specimens. Some cavities were found on the PAG boundaries, but they were not very numerous. For the detailed observation of the cavities, the specimens were fractured at liquid nitrogen temperature (LNT). As indicated by arrows, some small cavities clearly appear in the fractured surface. However, no cavities were observed in the specimen creep–fatigued within 0.8 N_f.

The identification of the precipitates by X-ray diffraction of the extracted precipitate residues is shown in Fig. 5. The precipitates were identified as $M_{23}C_6$ carbide and MX carbo-nitride for the as-tempered and fatigued specimens. Extensive studies have shown that there are two types of carbide, MX and $M_{23}C_6$, in modified 9Cr–1Mo steels [10,11]. To obtain a detailed understanding of the precipitates, the energy dispersive X-ray spectroscopy (EDS) and selected area diffraction (SAD) analysis were conducted as shown in Fig. 6. The equiaxed and elongated $M_{23}C_6$ carbides were presented in the form of chromium rich (Cr, Fe, Mo)$_{23}C_6$ and the remainder of the precipitates were the niobium and vanadium rich (NbV(CN)) type. Besides these precipitates, it has been reported that Laves Fe_2(Mo,W) phases nucleate on the martensite lath boundaries during long term aging [12], fatigue and creep deformation, and that these phases have a high growth rate, which is one of the major causes of the decrease of the creep strength [13,14]. However, no Laves phase was found in the 9Cr–1Mo–V–Nb steel during creep–fatigue at 550 °C.

Fig. 7 shows that the quantitative variation in the size of the precipitates, martensite lath width and Vickers hardness with the fatigue life fraction. The mean size of the precipitates increased very little and the total increase in the size of the precipitate was 10% or less. Many researchers have investigated the morphology, size distribution and compositional change of the precipitates during high temperature aging, fatigue and creep in 9%Cr steel. Cerri et al. [10] reported that MX and $M_{23}C_6$ carbide were coarsened during the creep of 9Cr–1Mo steel at 570–645 °C under stresses ranging from 85 MPa to 240 MPa. Okamura et al. [11] reported that the agglomeration and coarsening of the precipitates at the grain boundaries and lath interfaces was dominant during the long term creep of modified 9Cr–1Mo steel at 600 °C and 650 °C. However, they did not observe any coarsening of the precipitates during the fatigue test at 600 °C, because the fatigue test time was too short to cause any change in the precipitates. Sakasegawa et al. [13] studied the microstructural stability of ferritic 9%Cr steels under various external stresses, such as creep, fatigue and creep–fatigue. They did not observe any cyclic softening or coarsening of the precipitates during creep–fatigue at 400 °C. It is thus believed that the slight increase of the precipitate size during creep–fatigue

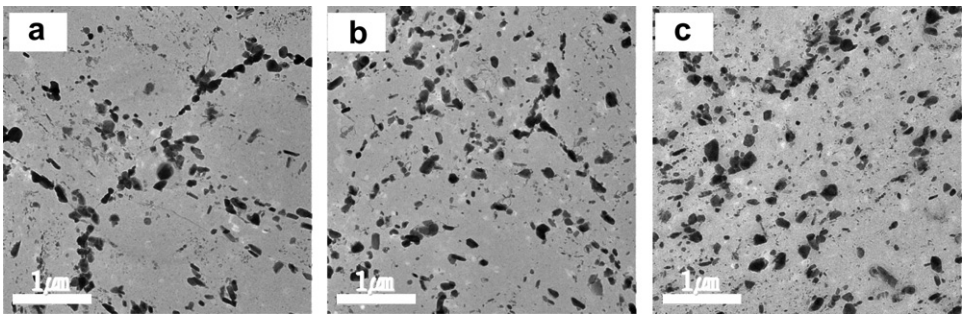

Fig. 2. TEM micrographs showing the precipitate morphology: (a) as-tempered, (b) $N/N_f = 1$, hold time of 60 s and (c) $N/N_f = 1$, hold time of 600 s.

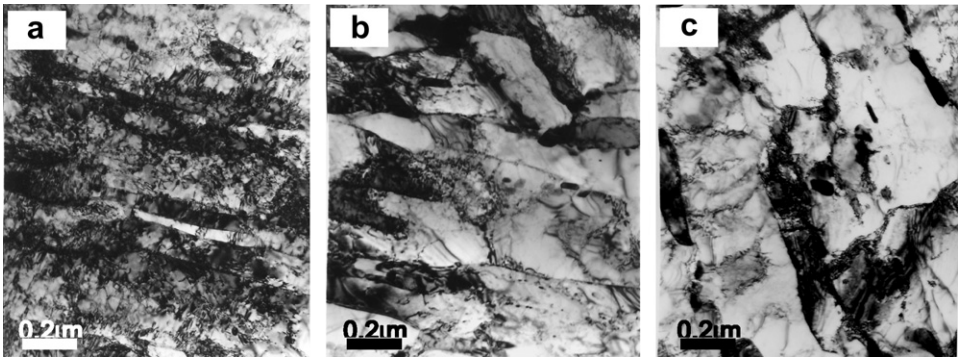

Fig. 3. TEM micrographs showing the dislocation substructure: (a) as-tempered, (b) $N/N_f = 1$, hold time of 60 s and (c) $N/N_f = 1$, hold time of 600 s.

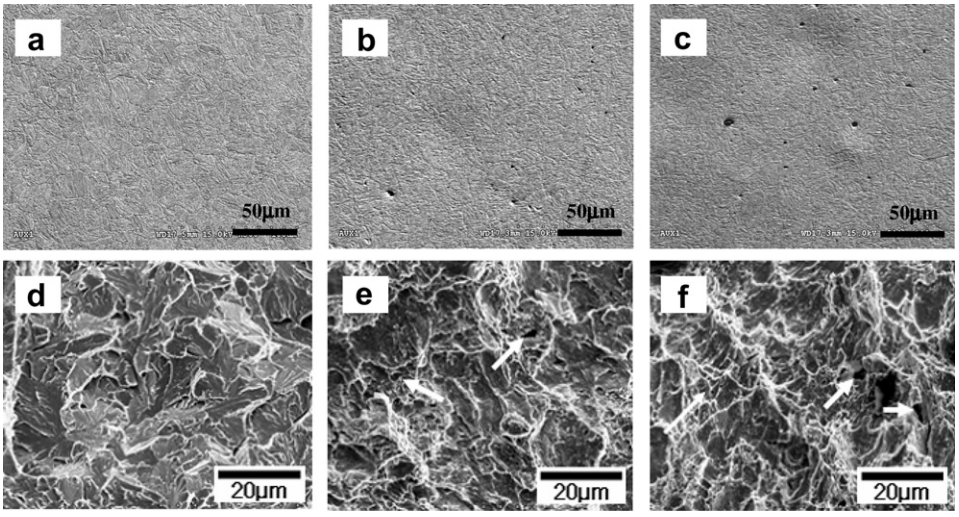

Fig. 4. BSE images of surface morphology and SEM micrographs showing the surface fractured at LNT: (a,d) as-tempered, (b,e) $N/N_f = 1$, hold time of 60 s, (c,f) $N/N_f = 1$, hold time of 600 s.

observed in this investigation can be attributed to the low temperature and short exposure time, as compared to the greater increase in the precipitate size observed after prolonged creep at high temperature in 9Cr–1Mo steel. The martensite lath width increased monotonously during creep–fatigue, as clearly show in the TEM micrographs of Fig. 3.

It is generally accepted that the increase of the lath width is due to the recovery of the dislocations within the lath boundaries and the recombination of the lath boundaries. Also, Abe [14] pointed out that the coarsening of the lath boundary in tempered 9Cr–W steel constituted the process of Y-junction movement. Therefore, the increase of the lath width is attributed to the movement of the Y-junction as well as to the recombination of the lath boundaries. The Vickers hardness decreased continuously accompanying the microstructural softening [15,16]. It was also noticed that the changes of the lath width, Vickers hardness and coarsening of the precipitates were more dominant in the case of the specimen with a holding time of 600 s than in that with a holding time of 60 s, indicating the importance of the holding time at the maximum tensile stress in the damage incurred by the fatigue. It is thought that the tensile hold time may have influence on cyclic life and life reduction of 9Cr–1Mo–V–Nb steel.

The dislocation density decreased during the creep–fatigue test, regardless of the fatigue hold time, as shown in Fig. 8. The disloca-

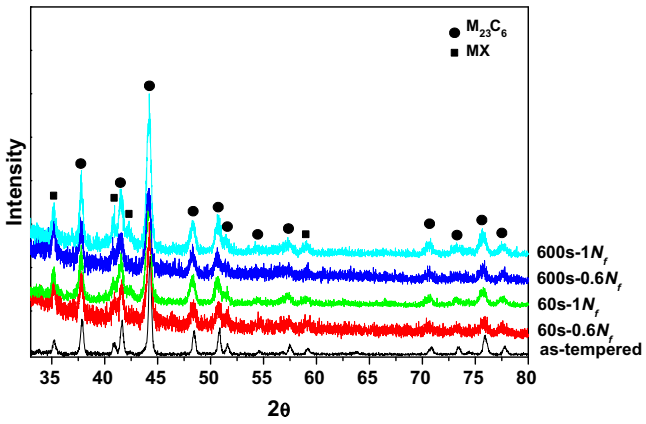

Fig. 5. X-ray diffraction profile of electrically extracted precipitates residues.

tion density decreased dominantly within 0.2 N_f, and then remained almost unchanged for the remaining part of the creep–fatigue life fraction.

4. Discussion

In general, the propagating velocity of a longitudinal wave, V_L, in a solid medium is given by the following equation:

$$V_L = \sqrt{\frac{K + \frac{4}{3}\mu}{\rho}} = \sqrt{\frac{E}{\rho}}\sqrt{\frac{(1-v)}{(1+v)(1-2v)}}, \quad (1)$$

where K is the bulk modulus, μ is the shear modulus, E is the Young's modulus, v is the Poisson's ratio and ρ is the bulk density.

As the above equation shows, the ultrasonic velocity is determined by the elastic modulus, the Poisson's ratio and the density of the material. Since the density and Poisson's ratio of a material can be assumed to remain constant during the creep–fatigue test until the cavity nucleates, the ultrasonic velocity is thought to be mainly dependent on the elastic modulus.

In the region within 0.2 N_f (region I), the ultrasonic velocity increased significantly. It is considered that the increase of the ultrasonic velocity is closely related to the dislocation density. Dislocations generally strain the lattice and interrupt the continuity of the matrix and, hence, they can lower the elastic modulus. Lee et al. [17] studied the microstructural effects (i.e. grain size, recovery, recrystallization, texture, etc.) on the elastic modulus using the sonic resonance test method. They reported that the elastic modulus increased during the recovery and recrystallization of copper alloy. Therefore, the increase in the ultrasonic velocity in region I occurs because the elastic modulus is increased due to the decrease in the dislocation density, as presented in Eq. (1). This result is in good agreement with previous studies [18,19]. For instance, Vasudevan et al. [18] claimed that the recovery during annealing can reduce the lattice distortion, resulting in an increase of the ultrasonic velocity.

In the region between 0.2 N_f and 0.8 N_f (region II), the ultrasonic velocity increased slightly. However, there was no change of the dislocation density measured by the X-ray diffraction method, as shown in Fig. 8. The main precipitate of the ferritic 9Cr–1Mo–V–Nb steel was $M_{23}C_6$ carbide containing solute atoms such as chromium and molybdenum. These solute atoms produce lattice distortion due to the difference in size between the dissolved solute atoms and the iron atoms. It was observed that the number of precipitates increased with creep–fatigue life fraction and the coarsening of precipitates occurred. This is thought to be closely related to the depletion of the solute atoms in the matrix [15,20] and, hence causes a decrease of the lattice distortion. Therefore, the slight increase of the ultrasonic velocity between the fatigue life fractions of 0.2 N_f and 0.8 N_f was attributed to the decrease of the lattice distortion due to the depletion of solute atoms from the matrix.

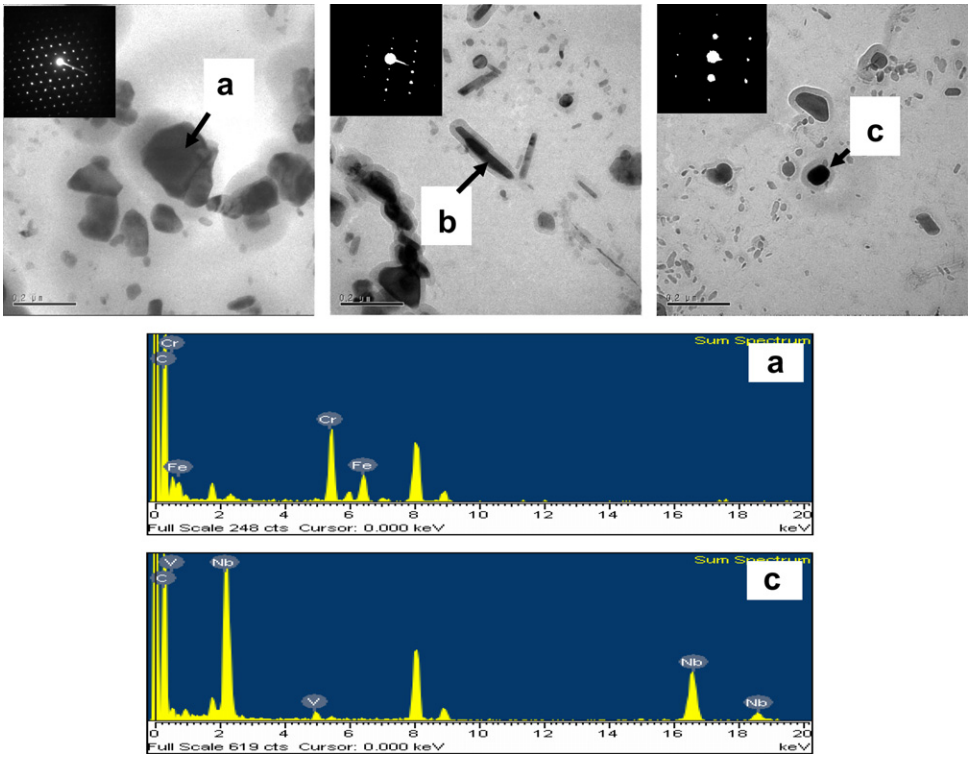

Fig. 6. TEM micrographs and SAD patterns of as-tempered specimen showing $M_{23}C_6$ and MX precipitates: (a) and (b) are $M_{23}C_6$ and (c) is MX.

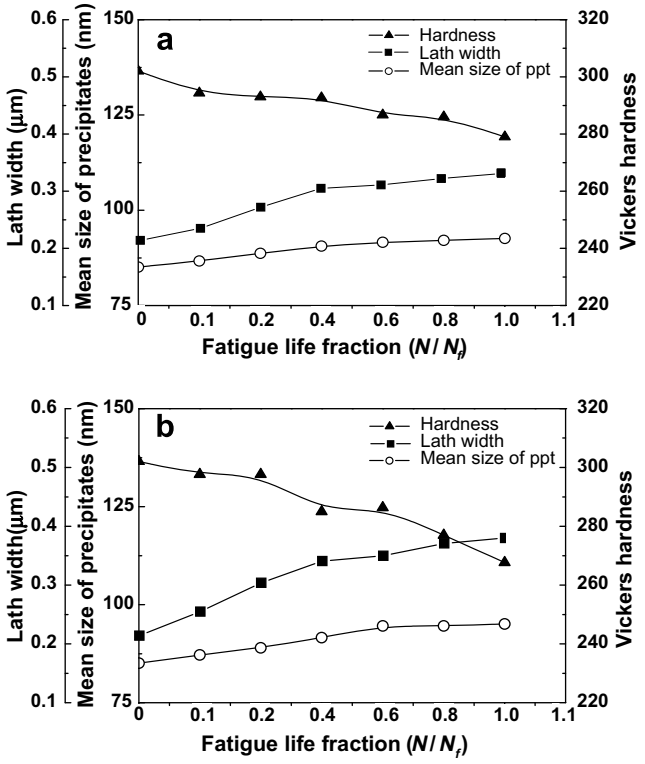

Fig. 7. Quantitative evaluation of microstructural changes with fatigue life fraction: (a) hold time of 60 s and (b) hold time of 600 s.

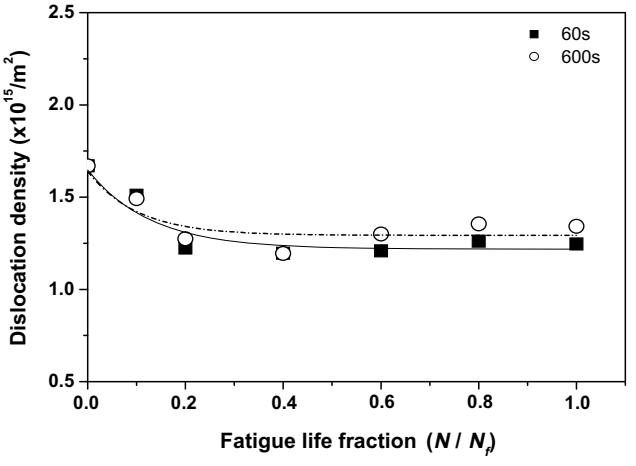

Fig. 8. Change of dislocation density with fatigue life fraction of ferritic 9Cr–1Mo–V–Nb steel.

In this study, the most typical microstructural change during the final stage of creep–fatigue (region III) was cavity formation, as shown in Fig. 4. Previous studies [21,22] have shown that there is a decrease of the ultrasonic velocity in creep damaged materials due to the formation of cavities inside them. The authors of these studies explained the decrease of the ultrasonic velocity afforded by cavity formation using the composite model. The composite model has been widely used to describe the effective physical properties, such as the effective elastic, thermal, and electrical properties, the volume of second phase (i.e. cavities having zero elastic stiffness). In this model, the elastic modulus decreases with increasing volume of the cavities. In this respect, the reduction of the ultrasonic wave velocity in the final stage is thought to be related to the decrease of the modulus due to cavity formation.

5. Conclusions

The ultrasonic velocity was observed to strongly depend on the microstructural changes during the creep–fatigue of ferritic 9Cr–1Mo–V–Nb steel. The ultrasonic velocity with the fatigue life fraction exhibited three distinct regions. In the first region ($N < 0.2\ N_f$), a significant increase in the velocity was observed. This increase was attributed to the decrease of the dislocation density, due to rearrangement and recovery. In the second region ($0.2\ N_f < N < 0.8\ N_f$), the ultrasonic velocity exhibited a slight increase due to the decrease of the lattice distortion caused by the depletion of solute atoms in the matrix. In the final region ($0.8\ N_f < N$), the ultrasonic velocity showed a slight decrease owing to the cavities generated during creep–fatigue.

Consequently, it was concluded that the degradation of 9Cr–1Mo–V–Nb steel subjected to creep–fatigue can be evaluated non-destructively by measuring the ultrasonic velocity.

Acknowledgment

This work was supported by a Korea University Grant.

References

[1] P.J. Ennis, A. Zielinska-Lipiec, O. Wachter, A. Czyrska-Filemonowicz, Acta Mater. 45 (1997) 4901.
[2] F. Abe, T. Horiuch, M. Taneike, K. Sawada, Mater. Sci. Eng. A 378 (2004) 299.
[3] G. Eggeler, J.C. Earthman, N. Nilsbang, B. Ilschner, Acta Metall. 37 (1989) 49.
[4] S. Luxenburger, W. Arnold, Ultrasonics 40 (2002) 797.
[5] G. Dobmann, M. Kroning, W. Theiner, H. Willems, U. Fiedler, Nucl. Eng. Des. 157 (1995) 137.
[6] S. Gupta, A. Ray, E. Keller, Int. J. Fatigue 29 (2007) 1100.
[7] C.S. Kim, S.I. Kwun, Mater. Trans. 48 (2007) 3028.
[8] C.S. Kim, I.H. Kim, I.K. Park, C.Y. Hyun, Key Eng. Mater. 326–328 (2006) 677.
[9] G.K. Williamson, W.H. Hall, Acta Metall. 1 (1953) 22.
[10] E. Cerri, E. Evangelista, S. Spigarelli, P. Bianchi, Mater. Sci. Eng. A 245 (1998) 285.
[11] H. Okamura, R. Ohtani, K. Saito, K. Kimura, R. Ishii, K. Fujiyama, S. Hongo, T. Iseki, H. Uchida, Nucl. Eng. Des. 193 (1999) 243.
[12] H. Sakasegawa, T. Hirose, A. Kohyama, Y. Katoh, T. Harada, K. Asakura, T. Kumagai, J. Nucl. Mater. 307–311 (2002) 490.
[13] H. Sakasegawa, T. Hirose, A. Kohyama, Y. Katoh, T. Harada, K. Asakura, Fus. Eng. Des. 61–62 (2002) 671.
[14] F. Abe, Mater. Sci. Eng. A 387–389 (2004) 565.
[15] M. Hattestrand, M. Schwind, H.O. Andren, Mater. Sci. Eng. A 250 (1998) 27.
[16] C.S. Kim, S.I. Kwun, B.Y. Ah, S.H. Nahm, S.S. Lee, Solid State Phenom. 118 (2006) 475.
[17] J.E. Lee, Y.C. Kim, J.P. Ahn, H.S. Kim, Acta Mater. 53 (2005) 129.
[18] M. Vasudevan, P. Palanichamy, S. Venkadesan, Scr. Metall. Mater. 30 (1994) 1479.
[19] P. Palanichamy, M. Vasudevan, T. Jayakumar, S. Venugopal, B. Raj, NDT&E Int. 33 (2000) 253.
[20] S. Saroja, P. Parameswaran, M. Vijayalakshmi, V.S. Raghunathan, Acta Metall. Mater. 43 (1995) 2985.
[21] T. Morishita, M. Hirao, Int. Solid Struct. 34 (1997) 1169.
[22] H. Jeong, D.H. Kim, Mater. Sci. Eng. A 337 (2002) 82.